Organic Electronics 13 (2012) 864–869

Contents lists available at SciVerse ScienceDirect

Organic Electronics

journal homepage: www.elsevier.com/locate/orgel

# Orientational control of pentacene crystals on $SiO_2$ by graphoepitaxy to improve lateral carrier transport

Shi-Guang Li [a,b,*], Naoki Nakayama [a], Masatoshi Sakai [a], Kazuhiro Kudo [a], Ryosuke Matsubara [b], Masakazu Nakamura [b,*]

[a] Department of Electrical and Electronic Engineering, Chiba University, 1-33 Yayoi-cho, Inage-ku, Chiba 263-8522, Japan
[b] Graduate School of Materials Science, Nara Institute of Science and Technology, 8916-5 Takayama, Ikoma, Nara 630-0192, Japan

ARTICLE INFO

*Article history:*
Received 6 October 2011
Received in revised form 11 January 2012
Accepted 29 January 2012
Available online 16 February 2012

*Keywords:*
Organic thin-film transistors
Pentacene
Graphoepitaxy
Grain boundaries
Periodic grooves

ABSTRACT

We controlled the in-plane orientation of pentacene grains by graphoepitaxy using patterned amorphous-$SiO_2$/Si substrates on which periodic grooves with slope edges had been formed. Pentacene crystals exhibited a clear tendency to align their *b*-axes perpendicular to the groove edges. Organic thin-film transistors were fabricated on the patterned and flat substrates and their transistor characteristics were compared. Although the patterned substrates increased the apparent mobility by only 10–20%, the number of grain boundaries with high potential barriers to carrier transport was reduced to half of that on flat substrates. This improvement is expected to enhance the response speed of pentacene organic thin-film transistors and suppress the sensitivity of their characteristics to the operating temperature.



## 1. Introduction

Organic thin-film transistors (OTFTs) have attracted great interest in recent years since they are suitable for the production of electronic circuits with low cost and low energy consumption, and can be used in flat, flexible large area electronic applications such as flat panel displays, electronic paper, large-area sensors, and low-cost radio frequency identification tags [1–6]. The characteristics of OTFTs have been greatly improved over the past decade. For single crystals, field-effect mobilities of up to 40 $cm^2$/Vs have been achieved [7], whereas field-effect mobilities of only about 1.0 $cm^2$/Vs have been reported for polycrystalline films, which are more important for practical applications. Grain boundaries in a polycrystalline active layer deteriorate the electrical performance of an OTFT because they generate potential barriers to carrier transport [8]. Such barriers not only reduce the apparent field-effect carrier mobility, they also determine the thermal activation energy for carrier transport and make the mobility very sensitive to the operating temperature. Potential barriers are predicted to be diminished once the oriented growth of grains is achieved [9,10]. However, organic thin films grown on amorphous surfaces such as $SiO_2$ or polymers inevitably consist of randomly oriented polycrystalline grains.

Several studies have found that pentacene [11,12], a typical organic material for OTFTs, or α-sexithiopene [13,14] tends to preferentially orient against sharp slope edges on substrates by graphoepitaxy. Graphoepitaxy is a phenomenon in which the macroscopic profile of the substrate surface restricts the orientation of growing crystals through the minimization of the free energy of crystals on the surface [15–19]. It is a promising technique for achieving oriented growth of crystalline films on amorphous substrates. If an array of such slope edges on the entire substrate surface cause all the grains to align in a

* Corresponding authors. Address: Graduate School of Materials Science, Nara Institute of Science and Technology, 8916-5 Takayama, Ikoma, Nara 630-0192, Japan. Tel./fax: +81 743 72 6125 (S.-G. Li), +81 743 72 6031 (M. Nakamura).

*E-mail addresses:* lisg@graduate.chiba-u.jp (S.-G. Li), mnakamura@ms.naist.jp (M. Nakamura).

1566-1199/$ - see front matter © 2012 Elsevier B.V. All rights reserved.
doi:10.1016/j.orgel.2012.01.027

single direction, then there are expected to be fewer grain boundaries with large potential barriers and consequently the field-effect carrier mobility is expected to increase.

In this study, we demonstrate control of the in-plane orientation of pentacene grains by fabricating periodic grooves with slope edges (patterned substrate). Pentacene crystals were grown on the substrates by vacuum deposition and their in-plane orientation angles relative to the slope edges were analyzed. We found that using the patterned substrates increased the mobility of patterned OTFTs by about 10–20%. Furthermore, both the in-plane orientation and the nucleation position of pentacene grains could be controlled to reduce the average barrier height of polycrystalline films.

## 2. Experimental

A heavily doped *n*-Si (1 0 0) wafer was used for the substrate and the gate electrode, while thermally oxidized $SiO_2$ (300 nm in thickness) served as a gate dielectric. Substrates with $SiO_2$ were sequentially cleaned in acetone, propanol, and deionized (DI) water and blown dry by $N_2$. A line-and-space photoresist pattern was formed on the substrate by conventional photolithography. The $SiO_2$ layer was etched in a buffered HF solution (see Fig. 1(a)). The grooves had a standard pitch of 3.5 μm and a depth of 20 nm. After stripping the photoresist, the partially completed device was cleaned using acetone and $UV/O_3$ (200 °C, 30 min) to remove surface contamination. The pentacene layer was deposited by vacuum deposition at a pressure of $2 \times 10^{-4}$ Pa. Growth rates were fixed to 3.0, 6.6, and 10.8 nm/min and the substrate temperature was varied in the range 40–80 °C. Average thicknesses of the pentacene film were 15 nm unless otherwise noted. Based on the results we obtained (Fig. 2), we performed experiments on OTFTs at the optimal deposition temperature of 60 °C. The OTFTs had a channel width of 5 mm and a length of 100 μm. Finally, Au electrodes were evaporated in vacuum using a shadow mask. The same procedure was used to fabricate flat OTFTs except that the photolithography and etching processes were omitted. The transistor characteristics were measured using a semiconductor parameter analyzer (Agilent Technologies, E5272A equipped with E5281A SMU). The average thickness of the grooved $SiO_2$ was used to calculate the field-effect carrier mobility of the patterned OTFTs. AFM (atomic force microscopy) images were obtained using a JEOL JSPM-5200 in tapping mode.

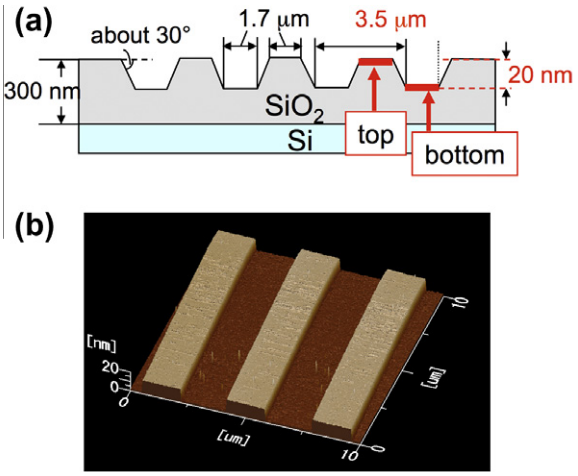


**Fig. 1.** (a) Cross-sectional view of the patterned substrate. (b) Three-dimensional view of AFM height image of patterned substrate.

## 3. Results and discussion

As shown in Fig. 2(a), many pyramidal grains were grown to make their peaks on the slope edge. The long axis of the pyramidal grain, or the bisector of an acute angle formed by two molecular steps as indicated in Fig. 2(a), corresponds to the *b*-axis of a pentacene grain [12]. Here, we denote the angle between the *b*-axis and the step edge as the in-plane orientation angle. We statistically analyzed the orientation distribution of hundreds of grains that are adjacent to the groove edge. Fig. 2(c–e) show the orientation distributions of pentacene grains grown at 40, 60, and 80 °C, respectively. As Fig. 2(c–e) show, the *b*-axes (i.e., the [0 1 0] direction) of pentacene grains grown on the groove edge have a strong tendency to be aligned perpendicular to the edge. This is clear evidence of the graphoepitaxy of pentacene crystals along the groove edges. The straight "folding line" of the substrate surface restricts the in-plane orientation of the pentacene nuclei by causing the [1 0 0]-direction molecular row to be parallel to the folding line in the initial stages of film growth [12]. Fig. 2(b) shows a typical AFM image of a very thin film where the pyramidal grains started their growth. In case of pentacene thin-film growth on a $SiO_2$ substrate, the first layer is known to grow in a different way from upper layers and nucleation of the second layer determines the final pyramidal structures [20]. As pointed out by arrows in Fig. 2(b), the nucleation of second layer tends to start from the slope edge with high probability. This must be due to trapping of migrating molecules at the slope edge. Because of this selective nucleation, the nuclei could become sensitive to the potential loss arising from the bending of crystal at the slope edge, and, as a result, higher degree of preferential orientation appears among the grains grown on the edge.

Of the tested samples, the highest degree of orientation was obtained at a growth temperature of 60 °C; 49% of the grains were aligned in the orientation angle range 80–100°. Increasing substrate temperature generally accelerates the competition of the growth among differently oriented grains and promotes the influence of graphoepitaxy. However, at the same time, thermal motion of molecules would vanish the difference of free energy between differently oriented grains when growth temperature is too high. Consequently, an optimum growth temperature was 60 °C in the current system. In the subsequent experiments, growth temperature of 60 °C was therefore adopted to form orientation-controlled films.

Fig. 3(a–f) show AFM height images of pentacene grains grown on patterned and flat $SiO_2$ substrates, respectively. In

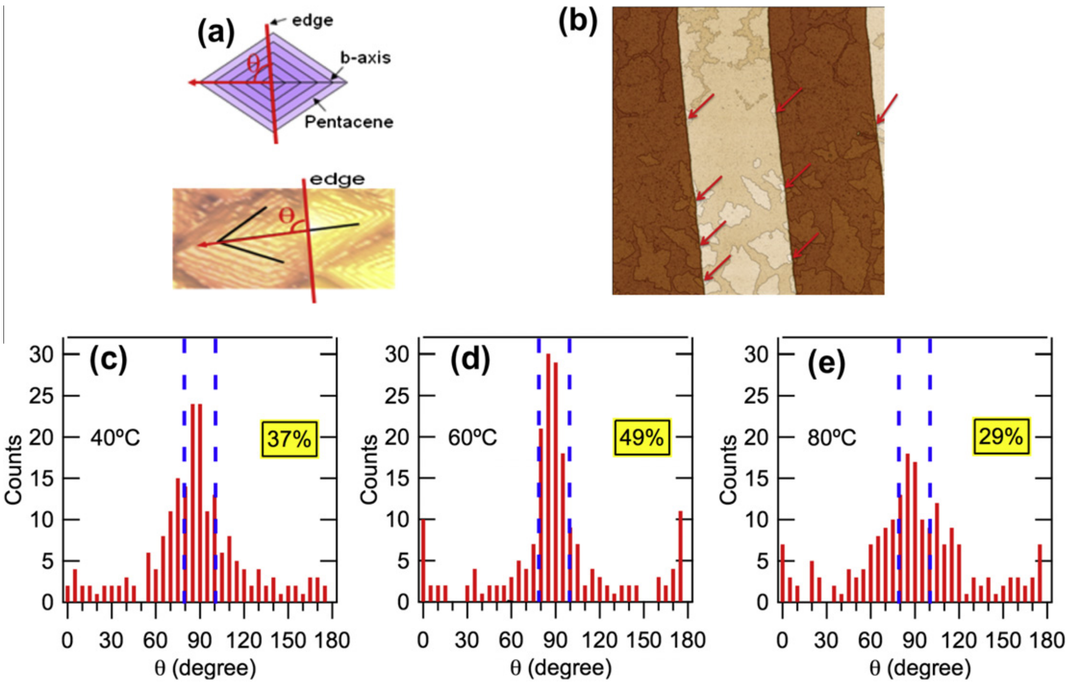


**Fig. 2.** (a) Definition of the orientation angle of *b*-axis relative to the groove edge, (b) typical AFM height image taken at the initial stage of film growth, and (c–e) histograms showing orientation distribution of pentacene grains (average thickness: 15 nm) adjacent to groove edges grown at (c) 40, (d) 60, and (e) 80 °C. The arrows in (b) indicate pyramidal grains that start their growth from the slope edge. The dashed lines in (c–e) indicate the angle range 80–100°.

this experiment, growth rates of 3.3, 6.6, and 10.8 nm/min were used; at each growth rate, pentacene films were simultaneously deposited onto a pair of patterned and flat substrates, which were set in a sample holder that was rotated during deposition. Au top-contact electrodes were also simultaneously deposited on the pair of patterned and flat substrates. In contrast with the random appearance of the grains in the flat OTFTs, the grains on the patterned OTFTs exhibit relatively well-ordered grain shapes and nuclei positions due to the groove edge. Fig. 3(g–i) show the transfer curves of the pentacene OTFTs; the red and blue lines are the transfer curves of the patterned and flat OTFTs, respectively. Table 1 lists the field-effect mobilities calculated from Fig. 3(g–i). For the patterned OTFTs, average thickness of $SiO_2$ layer is used to calculate the mobilities, and the error due to the dielectric thickness is therefore expected to be less than 1%. At any deposition rate, a patterned OTFT has about a 10–20% higher mobility than the corresponding flat OTFT, of which difference is significant enough for the careful comparative experiment in this work.

Based on the values given in Table 1, the use of a patterned substrate may seem to cause a minor improvement in the mobility. However, the mobility of pentacene polycrystalline films also depends on the grain size of the film and the patterned substrates apparently have smaller average grain sizes than flat substrates (see Fig. 3(a–f)). It is thus important to account for the influence of grain size when evaluating the reduction in the potential barriers at grain boundaries by the in-plane orientation of grains. In previous studies [8,21,22], we found that the apparent mobility of a polycrystalline pentacene film can be described by:

$$\mu = \frac{ql}{2k_BT}\mu_h\sqrt{\frac{qN_A\Phi_b}{2\epsilon_s}}\exp\left(-\frac{q\Phi_b}{2\epsilon_s}\right) \quad (1)$$

where $q\Phi_b$ is the average barrier height at grain boundaries, $l$ is the average grain size, $\mu_h$ is the mobility in the grain (which depends on the very small potential fluctuation in the grain [21]), and $N_A$ is the acceptor density. According to Eq. (1), the apparent mobility of pentacene polycrystalline films is proportional to the grain size when the other parameters (including the barrier height) are constant.

In Fig. 4, mobility values obtained in this work are plotted against average grain size. For this analysis, the average grain size of pentacene on a patterned substrate was measured parallel to the direction of current flow. Data points in Fig. 4 are apparently separated into two groups depending on the substrate. We therefore tried to estimate average $\Phi_b$ for each group. Fitting Eq. (1) to the experimental data by varying $\Phi_b$ and setting the other parameters to those used in our previous study [8], the flat and patterned OTFTs were estimated to have average barrier heights of 157 and 132 meV, respectively. Thus, the average barrier height is clearly reduced when the pentacene grains are aligned in a single direction determined by the array of slope edges. At room temperature, the reduction in the barrier height corresponds to a 2.1-fold increase in the apparent mobility when the other parameters (including the grain size) remain unchanged.

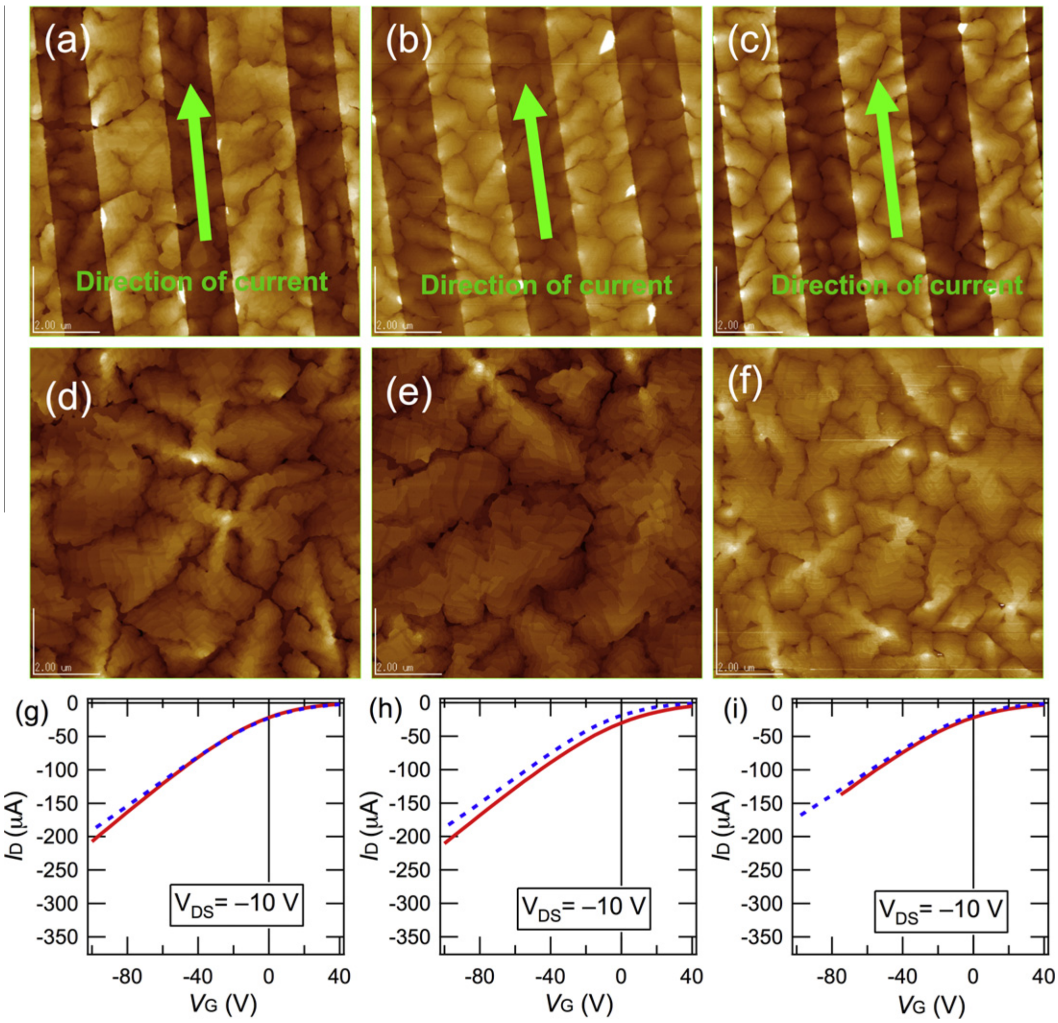


**Fig. 3.** AFM height images (10 × 10 μm$^2$) of pentacene grains grown at 60 °C on (a–c) patterned and (d–f) flat $SiO_2$ substrates and (g–i) transfer curves of the OTFTs with the pentacene films in (a–f). The pentacene film growth rate was maintained at (a, d, g) 3.3, (b, e, h) 6.6, and (c, f, i) 10.8 nm/min. Solid and dashed lines in (g–i), respectively indicate transfer curves of patterned and flat OTFTs measured at $V_{DS} = -10$ (V).

**Table 1**
Mobilities of pentacene in patterned and flat OTFTs at three growth rates.

| Growth rate (nm/min) | Mobility (cm$^2$/Vs) | | Increase of mobility |
|---|---|---|---|
| | Patterned | Flat | |
| 3 | 0.38 | 0.32 | +19% |
| 6.6 | 0.36 | 0.31 | +16% |
| 10.8 | 0.31 | 0.28 | +11% |

Here, we discuss how the patterned substrate influences the apparent mobility. The patterned substrate reduced the average barrier height from 157 to 132 meV. If we assume that the orientational control causes some grain boundaries to become barrierless while the other grain boundaries remain unchanged, the ratio of the additional barrierless boundaries is calculated to be 58% from Eq. (1) (i.e., approximately half the boundary barriers are reduced). On the other hand, we estimate that 49% of the grains are oriented nearly perpendicular to the groove edge based on the orientation distribution in Fig. 2(c). From this ratio, 24% of the grain boundaries that appear along the groove direction (the same direction as the current flow) are expected to become additional small-misfit-angle grain boundaries. If a twin boundary between two perfect crystals is in concern, a small misfit angle may induce a higher potential barrier. However, it is known that a crystal grain of pentacene grown on $SiO_2$ is composed of (25–50)-nm-sized crystallites [23], which means that the boundary of interest is composed of many nano-boundaries having a narrow, but not negligible, distribution of local misfit angle. In such a case, small macroscopic misfit angle or a phase shift of molecular lattice will not drastically change the macroscopic transport barriers because local current path, where nano-boundaries are nearly ideal for lattice fusion, dominates the carrier transport across the boundary. As a consequence, the additional small-misfit-angle grain boundaries are expected to have much lower barrier height.

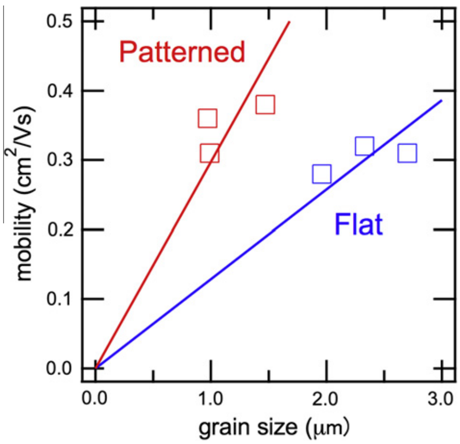


**Fig. 4.** Field-effect mobilities of (red) patterned and (blue) flat OTFTs plotted against average grain size. (For interpretation of the references to color in this figure legend, the reader is referred to the web version of this article.)

Fig. 5 shows an AFM height image of pentacene grains in the patterned OTFT (growth rate: 6.6 nm/min). From four similar images taken on different locations, we determined that about 28% of the grain boundaries have small-misfit-angles. This ratio agrees well with the expected probability from the orientation distribution. However, it is much smaller than the ratio of additional barrierless boundaries, 58%, which is estimated from the grain size dependence of the mobility. There must therefore be another factor that reduces the high-barrier boundary. Comparison of the AFM images in Fig. 3 reveals that grain boundaries along the groove edge are thicker or morphologically better connected than other grain boundaries. This is due to the alignment of the growth nuclei on the groove edge. This would cause the in-plane orientation to reduce the average barrier height more than expected. Consequently, the patterned substrate is considered to affect the apparent mobility of pentacene polycrystalline films not only by the controlled orientation of the grains but also by alignment of the grains along the current direction.

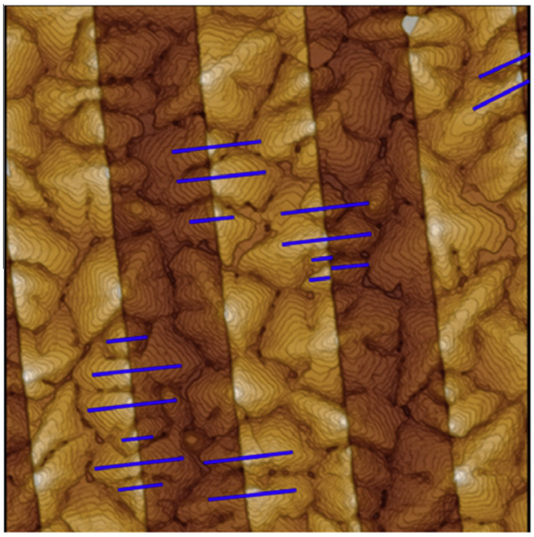

**Fig. 5.** AFM height image ($10 \times 10\ \mu m^2$) of pentacene grains grown at 60 °C and 6.6 nm/min on patterned substrates. A high-pass-filtered image is combined with the corresponding color-scale image to enhance the shape of the molecular steps. Blue lines indicate parallel in-plane orientation of adjacent pentacene grains. (For interpretation of the references to color in this figure legend, the reader is referred to the web version of this article.)

## 4. Conclusions

We demonstrated that the in-plane orientation of pentacene grains could be controlled by using periodic grooves with slope edge structures. Nearly half the grains were aligned so that their *b*-axes were perpendicular to the groove edge. Compared to flat OTFTs, the patterned OTFTs had a 10–20% higher field-effect mobility. This increase in the mobility is relatively small because the average grain size decreases when a patterned substrate is used and when the deposition conditions remain the same. By accounting for the influence of grain size, the average barrier height at grain boundaries in the patterned OTFTs was considerably smaller (132 meV) than that in the flat ones (157 meV). The mobility could be further improved by optimizing the deposition conditions for the patterned substrate. On the other hand, the number of large-barrier grain boundaries was estimated to be reduced more than that expected based on the grain orientation distribution. The influence of the patterned substrate must therefore be caused not only by the controlled orientation of the grains but also by the alignment of the grains along the current direction. The present results imply that all mobility-determining factors (i.e., the in-plane orientation, size, and alignment of grains) should be considered when discussing the influence of patterned substrates on transistor characteristics.

## Acknowledgements

This study was supported by a Grant-in-Aid for Scientific Research (B) (No. 21350099), the Chiba University Global COE Program "Advanced School for Organic Electronics", and a Grant-in-Aid for JSPS Fellows (No. 23-56142).

## References

[1] B. Crone, A. Dodabalapur, Y.-Y. Lin, R.W. Filas, Z. Bao, A. LaDuca, R. Sarpeshkar, H.E. Katz, W. Li, Nature 403 (2000) 521.
[2] V. Subramanian, P.C. Chang, J.B. Lee, S.E. Molesa, S.K. Volkman, IEEE Trans. Compon. Packag. Technol. 28 (2005) 742.
[3] E. Cantatore, T.C.T. Geuns, G.H. Gelinck, E. van Veenendaal, A.F.A. Gruijthuijsen, L. Schrijnemakers, S. Drews, D.M. de Leeuw, IEEE J. Solid-State Circuits 42 (2007) 84.
[4] L. Zhou, A. Wanga, S.-C. Wu, J. Sun, S. Park, T.N. Jackson, Appl. Phys. Lett. 88 (2006) 083502.
[5] J.A. Rogers, Z. Bao, K. Baldwin, A. Dodabalapur, B. Crone, V.R. Raju, V. Kuck, H. Katz, K. Amundson, J. Ewing, P. Drzaic, Proc. Natl. Acad. Sci. USA 98 (2001) 4835.
[6] A.N. Sokolov, M.E. Roberts, Z. Bao, Mater. Today 12 (2009) 12.
[7] O.D. Jurchescu, M. Popinciuc, B.J. van Wees, T.T.M. Palstra, Adv. Mater. 19 (2007) 688.

[8] R. Matsubara, N. Ohashi, M. Sakai, K. Kudo, M. Nakamura, Appl. Phys. Lett. 92 (2008) 242108.
[9] A.B. Chwang, C.D. Frisbie, J. Appl. Phys. 90 (2001) 1342.
[10] M. Nakamura, T. Matsunobe, H. Tokumoto, J. Appl. Phys. 89 (2001) 7860.
[11] Y. Hattori, M. Kubata, T. Uemiya, G. Tanaka, Jpn. J. Appl. Phys. 34 (1995) 3871.
[12] M.-S. Xu, M. Nakamura, M. Sakai, K. Kudo, Adv. Mater. 19 (2007) 371.
[13] S. Ikeda, K. Saiki, K. Tsutsui, T. Edura, Y. Wada, H. Miyazoe, K. Terashima, K. Inaba, T. Mitsunaga, T. Shimada, Appl. Phys. Lett. 88 (2006) 251905.
[14] S. Ikeda, K. Saiki, Y. Wada, K. Inaba, Y. Ito, H. Kikuchi, K. Terashima, T. Shimada, J. Appl. Phys. 103 (2008) 084313.
[15] H.I. Smith, D.C. Flanders, Appl. Phys. Lett. 32 (1978) 349.
[16] K. Kushida, H. Takeuchi, T. Kobayashi, K. Takagi, Appl. Phys. Lett. 48 (1986) 764.
[17] E.I. Givargizov, Thin Solid Films 189 (1990) 389.
[18] Y. Wada, T. Kobayashi, T. Kure, T. Yoshimura, Y. Sudou, Y. Gotou, S. Kondo, J. Electrochem. Soc. 141 (1994) 1392.
[19] A.L. Giermann, C.V. Thompson, Appl. Phys. Lett. 86 (2005) 121903.
[20] K. Puntambekar, J. Dong, G. Haugstad, C.D. Frisbie, Adv. Funct. Mater. 16 (2006) 879.
[21] N. Ohashi, H. Tomii, R. Matsubara, M. Sakai, K. Kudo, M. Nakamura, Appl. Phys. Lett. 91 (2007) 162105.
[22] M. Nakamura, H. Ohguri, N. Goto, H. Tomii, M.-S. Xu, T. Miyamoto, R. Matsubara, N. Ohashi, M. Sakai, K. Kudo, Appl. Phys. A 95 (2009) 73.
[23] R. Matsubara, M. Sakai, K. Kudo, N. Yoshimoto, I. Hirosawa, M. Nakamura, Org. Electron. 12 (2011) 195.